

## SU(4) Kondo Effect in Carbon Nanotubes

Manh-Soo Choi,<sup>1</sup> Rosa López,<sup>2,3</sup> and Ramón Aguado<sup>4</sup>

<sup>1</sup>*Department of Physics, Korea University, Seoul 136-701, Korea*

<sup>2</sup>*Département de Physique Théorique, Université de Genève, CH-1211 Genève 4, Switzerland*

<sup>3</sup>*Department de Física, Universitat de les Illes Balears, E-07122 Palma de Mallorca, Spain*

<sup>4</sup>*Teoría de la Materia Condensada, Instituto de Ciencia de Materiales de Madrid (CSIC) Cantoblanco, 28049 Madrid, Spain*

(Received 18 October 2004; published 5 August 2005)

We investigate theoretically the nonequilibrium transport properties of carbon nanotube quantum dots. Owing to the two-dimensional band structure of graphene, a double orbital degeneracy plays the role of a pseudospin, which is entangled with the spin. Quantum fluctuations between these 4 degrees of freedom result in an SU(4) Kondo effect at low temperatures. This exotic Kondo effect manifests as a four-peak splitting in the nonlinear conductance when an axial magnetic field is applied.

DOI: 10.1103/PhysRevLett.95.067204

PACS numbers: 75.20.Hr, 72.15.Qm, 73.63.Fg

**Introduction.**—Carbon nanotubes (NTs) exhibit a good deal of remarkable transport phenomena, including quantum interference [1], Luttinger liquid features [2], or spin polarized transport [3]. Finite-length NTs behave as quantum dots (QDs) and thus show Coulomb blockade [4,5] and Kondo physics [6]. Interestingly, the richness of the band structure of NTs and the feasibility to attach new materials as electrodes, e.g., ferromagnetic [3] or superconducting contacts [7], allows us to explore new aspects of the Kondo effect, one of the central topics in condensed matter physics.

The electronic states of a NT form one-dimensional electron and hole subbands. They originate from the quantization of the electron wave number perpendicular to the nanotube axis,  $k_{\perp}$ , which arises when graphene is wrapped into a cylinder to create a NT. By symmetry, for a given subband at  $k_{\perp} = k_0$  there is a second degenerate subband at  $k_{\perp} = -k_0$ . Semiclassically, this orbital degeneracy corresponds to the clockwise ( $\cup$ ) or counterclockwise ( $\oslash$ ) symmetry of the wrapping modes.

In this Letter, we combine several theoretical approaches, scaling theory, numerical renormalization group (NRG) [8], noncrossing approximation (NCA) [9], equation-of-motion (EOM) [10] methods, to present a unified picture of low-temperature, nonequilibrium transport through NTQDs in the presence of magnetic fields. We show that quantum fluctuations between the four states  $\{\cup \uparrow, \cup \downarrow, \oslash \uparrow, \oslash \downarrow\}$  may dominate transport at low temperatures provided that both the orbital and spin indexes are conserved during tunneling. This leads to a highly symmetric SU(4) Kondo effect, and hence an enhanced Kondo temperature, in which the spin and the orbital degrees of freedom are totally entangled [11]. We also point out that the orbital degeneracy in the dot itself is not enough for having SU(4) Kondo physics. In general, SU(2) Kondo physics is possible. We show that neither an enhanced Kondo temperature nor linear conductance measurements can distinguish between the two effects. Instead, the nonlinear conductance in the presence of a *parallel* magnetic field shows a four-peak structure, with different splittings for the

spin and the orbital sectors, which unambiguously signals SU(4) Kondo physics. Our theoretical results are in good agreement with recent experiments by Jarillo-Herrero *et al.* [12].

**Model.**—We study a NTQD coupled to left ( $L$ ) and right ( $R$ ) electrodes. We consider the case where the NTQD has two (nearly) degenerate localized orbitals [labeled by the quantum number  $m = 1, 2$ , where 1 (2) denotes  $\cup$  ( $\oslash$ ) orbital mode]. The presence of an axial magnetic field ( $B_{\parallel}$ ) lifts *both* the orbital and the spin degeneracies: A parallel magnetic field induces an Aharonov-Bohm phase  $2\pi\Phi/\Phi_0$ , where  $\Phi = \pi d_t^2/4B_{\parallel}$  is the flux threading the NT,  $\Phi_0 = h/e$  is the flux quantum, and  $d_t$  the tube diameter. This Aharonov-Bohm flux shifts the allowed  $k_{\perp}$ , and the orbital degeneracy is lifted by an amount  $\pm\Delta_{\text{orb}} = \pm ed_t v_F B_{\parallel}/4$ , where  $v_F$  is the Fermi velocity [13]. The states near the energy gap correspond to semiclassical orbits which have an *orbital* magnetic moment  $\mu_{\text{orb}} = ed_t v_F/4$ . Thus, an axial magnetic field leads to an energy shift  $\Delta_{\text{orb}} = \mu_{\text{orb}} B_{\parallel}$ . The states further split due to the Zeeman energy  $\pm\Delta_Z/2 = \pm g\mu_B B_{\parallel}/2$ , where  $\mu_B$  is the Bohr magneton and  $g \approx 2$  is the  $g$  factor in nanotubes.  $\mu_{\text{orb}}$  scales with the NT diameter and is typically 1 order of magnitude larger than the Bohr magneton [12,14], resulting in a stronger influence of  $B_{\parallel}$  on the orbital sector. Thus, the single particle energy  $\epsilon_{m\sigma}$  associated with the orbital  $m$  and the spin  $\sigma$  is given by  $\epsilon_{m\sigma} = \epsilon_d + \Delta_{\text{orb}}(\delta_{m,1} - \delta_{m,2}) + (\Delta_Z/2)(\delta_{\sigma,\uparrow} - \delta_{\sigma,\downarrow})$ . The NTQD is then described by the Hamiltonian

$$\mathcal{H}_D = \sum_{m=1,2} \sum_{\sigma=\uparrow,\downarrow} \epsilon_{m\sigma} d_{m,\sigma}^{\dagger} d_{m,\sigma} + \frac{1}{2} U (n - n_g)^2, \quad (1)$$

where  $n = \sum_{m,\sigma} d_{m,\sigma}^{\dagger} d_{m,\sigma}$  is the occupation and  $U$  is the Hubbard-like on-site interaction (we focus on the regime where the QD is occupied by a single electron). The two leads are modeled as

$$\mathcal{H}_C = \sum_{\alpha \in L,R} \sum_{m=1,2} \sum_{k,\sigma} \epsilon_{\alpha,k} c_{\alpha,k,m,\sigma}^{\dagger} c_{\alpha,k,m,\sigma} \quad (2)$$

Without loss of generality, we assume that there are two distinguished (groups of) channels  $m = 1, 2$  in each lead [15]. The coupling between the leads and the NTQD is described by the tunneling Hamiltonian

$$\mathcal{H}_T = \sum_{\alpha,k,\sigma} \sum_{m,m'} V_{m,m'}^\alpha (c_{\alpha,k,m,\sigma}^\dagger d_{m',\sigma} + \text{H.c.}), \quad (3)$$

where the tunneling amplitudes read  $V_{m,m'}^\alpha = [V_0 \delta_{m,m'} + V_X(1 - \delta_{m,m'})]/\sqrt{2}$  (for simplicity, we ignore their  $k$  and  $\sigma$  dependence). In the most general case, they describe two types of tunneling processes: (i) those in which the orbital quantum number is conserved, denoted by  $V_{1,1}^\alpha = V_{2,2}^\alpha = V_0/\sqrt{2}$  and (ii) those events accounting for mixing (cross coupling)  $V_{m,m'}^\alpha = V_X/\sqrt{2}$  with  $m \neq m'$ . To gain more physical intuition when  $V_X \neq 0$  we rewrite the total Hamiltonian  $\mathcal{H} = \mathcal{H}_D + \mathcal{H}_C + \mathcal{H}_T$  in terms of symmetric (even) and antisymmetric (odd) combinations of the orbital channels. First, we simplify the algebra by performing a canonical transformation,  $c_{L(R),k,m,\sigma} = (a_{k,m,\sigma} \pm b_{k,m,\sigma})/\sqrt{2}$ , such that the resulting Hamiltonian contains only a single lead,  $a_{k,m,\sigma} = (c_{L,k,m,\sigma} + c_{R,k,m,\sigma})/\sqrt{2}$ , with two channels  $m = 1, 2$ . Next, we apply the even-odd transformation  $a_{k,1(2),\sigma} = (c_{k\sigma} \pm ic_{k_o\sigma})/\sqrt{2}$  and  $d_{1(2)\sigma} = (d_{e\sigma} \pm id_{o\sigma})/\sqrt{2}$ , such that  $\mathcal{H}$  reads

$$\begin{aligned} \mathcal{H} = & \sum_{\sigma,\nu=e,o} \epsilon_{k\nu} c_{k\nu,\sigma}^\dagger c_{k\nu,\sigma} + \sum_{\sigma,\nu=e,o} \epsilon_{\nu\sigma} d_{\nu,\sigma}^\dagger d_{\nu,\sigma} \\ & + U(n - n_g) + \sum_{\nu=e,o} \sum_{k\nu,\sigma} V^\nu (c_{k\nu,\sigma}^\dagger d_{\nu\sigma} + \text{H.c.}), \quad (4) \end{aligned}$$

with  $V^e \equiv V_0 + V_X$  and  $V^o \equiv V_0 - V_X$  (note that  $\epsilon_{k\nu}$  and  $\epsilon_{\nu\sigma}$  remain invariant under this transformation). When  $V_X = 0$ , both the even and odd orbitals are equally coupled to the NTQD ( $V^e = V^o = V_0$ ). Thus, at small energies the effective model leads to SU(4) Kondo physics; see below. However, for the maximal mixing, i.e.,  $V_X = V_0$ , the even orbital is doubly coupled ( $V^e = 2V_0$ ), whereas the odd orbital becomes *uncoupled* ( $V^o = 0$ ). Here, SU(2) Kondo physics arises owing to spin fluctuations in the even orbital channel. Here, for simplicity, we have discussed the two limiting cases only. In the more general case, we obtain a crossover from SU(4) to SU(2) symmetry as the ratio  $V_X/V_0$  increases [16].

*Effective Kondo model.*—Let us now substantiate our previous arguments by examining the low-energy properties of the system. After performing a Schrieffer-Wolf transformation to  $\mathcal{H}$ , the effective Hamiltonian reads

$$\begin{aligned} \mathcal{H}_K = & \mathcal{H}_C + \frac{J_1}{4} [\mathbf{S} \cdot (\psi^\dagger \boldsymbol{\sigma} \psi) + \mathbf{S} \cdot (\psi^\dagger \boldsymbol{\sigma} \tau^z \psi) T^x] \\ & + \frac{J_2}{4} [\mathbf{S} \cdot (\psi^\dagger \boldsymbol{\sigma} \boldsymbol{\tau}^\perp \psi) \cdot \mathbf{T}^\perp + (\psi^\dagger \boldsymbol{\tau}^\perp \psi) \cdot \mathbf{T}^\perp] \\ & + \frac{J_3}{4} (\psi^\dagger \tau^z \psi) T^x + \frac{J_4}{4} [\mathbf{S} \cdot (\psi^\dagger \boldsymbol{\sigma} \tau^z \psi) \\ & + \mathbf{S} \cdot (\psi^\dagger \boldsymbol{\sigma} \psi) T^x] - J_5 T^x + \mu_{BG} \mathbf{B} \cdot \mathbf{S} + \mu_{\text{orb}} \mathbf{B} \cdot \mathbf{T}, \quad (5) \end{aligned}$$

where  $\psi_k^\dagger = [c_{k,e,\uparrow}^\dagger c_{k,e,\downarrow}^\dagger c_{k,o,\uparrow}^\dagger c_{k,o,\downarrow}^\dagger]$  are the field operators for the leads in the even-odd basis and  $\psi = \sum_k \psi_k$ . The field operator for the NTQD  $\psi_d^\dagger = [d_{e,\uparrow}^\dagger d_{e,\downarrow}^\dagger d_{o,\uparrow}^\dagger d_{o,\downarrow}^\dagger]$  defines the orbital pseudospin and the spin operators given by  $\mathbf{T} = \psi_d^\dagger \boldsymbol{\tau} \psi_d$  and  $\mathbf{S} = \psi_d^\dagger \boldsymbol{\sigma} \psi_d$ , respectively, with  $\tau$  and  $\sigma$  being the Pauli matrices in the orbital pseudospin and spin spaces, respectively. Here,  $T^\perp (\boldsymbol{\tau}^\perp)$  denotes  $T^y + T^z (\boldsymbol{\tau}^y + \boldsymbol{\tau}^z)$ . Using renormalization group (RG) arguments, the effective coupling constants in the  $U$ -large limit are given initially by  $J_1 = J_3 = \mathcal{N} V^2 / \epsilon_d$ ,  $J_2 = J_1 (|V_0|^2 - |V_X|^2) / V^2$ , and  $J_4 = J_1 |2V_0 V_X| / V^2$ , where  $V^2 = |V_0|^2 + |V_X|^2$  ( $\mathcal{N}$  is the degeneracy).  $J_5$  is not renormalized in the RG procedure and does not flow into the strong coupling regime. At zero magnetic field with only spin and orbital conserving tunneling processes ( $V_X = 0$ ),  $J_1 = J_2 = J_3 = J$  while  $J_4 = J_5 = 0$ . The corresponding Hamiltonian is reduced to the SU( $\mathcal{N} = 4$ ) Kondo model where the spin  $\mathbf{S}$  and the orbital pseudospin  $\mathbf{T}$  are entangled (last term of the equation),

$$\begin{aligned} \mathcal{H}_{\text{SU}(4)} = & \mathcal{H}_C + (J/4) [\mathbf{S} \cdot (\psi^\dagger \boldsymbol{\sigma} \psi) \\ & + (\psi^\dagger \boldsymbol{\tau} \psi) \cdot \mathbf{T} + \mathbf{S} \cdot (\psi^\dagger \boldsymbol{\sigma} \boldsymbol{\tau} \psi) \cdot \mathbf{T}]. \quad (6) \end{aligned}$$

The scaling equations are reduced to a single equation:

$$dJ/d \ln D = -\mathcal{N} \rho_0 J^2, \quad (7)$$

where  $\rho_0$  is the density of states (DOS) in the leads and  $D$  is the bandwidth, resulting in the exponentially enhanced Kondo temperature  $T_K^{\text{SU}(4)} \approx D \exp[-1/(\mathcal{N} \rho_0 J)]$  compared with  $T_K^{\text{SU}(2)}$  of the single-level SU( $\mathcal{N} = 2$ ) model.

In the other limiting case ( $V_X = V_0$ ), the corresponding Kondo-like Hamiltonian [Eq. (5) at  $B = 0$  with  $J_1 = J_3 = J_4 = 2\mathcal{N}|V_0|^2/\epsilon_d$  and  $J_2 = 0$ ] involves only spin fluctuations in the doubly degenerate ( $\mathcal{N} = 2$ ) even orbital. It gives rise to what we call a two-level (TL) SU(2) model:  $\mathcal{H}_{\text{TL SU}(2)} = \mathcal{H}_C + J \mathbf{S}_e \cdot (\psi_e^\dagger \boldsymbol{\sigma} \psi_e) (1 + T^x) + (J/4) \times (\psi_e^\dagger \psi_e) T^x - J_5 T^x$ . The RG equation for  $J$  is

$$dJ/d \ln D = -2\mathcal{N} \rho_0 J^2. \quad (8)$$

This model corresponds to an SU(2) Fermi liquid [17] with a Kondo temperature  $T_K^{\text{TL SU}(2)}$  which is *the same* as  $T_K^{\text{SU}(4)}$  [compare Eqs. (7) and (8); the factor 2 comes from the doubling of the coupling  $2V_0$  [18]].

The scaling arguments above are confirmed by the NRG studies of the spectral density  $A_{m\sigma}(\omega)$  for the localized level  $m\sigma$ . At  $B_{\parallel} = 0$ , the spectral density shows a peak near the Fermi energy, corresponding to the formation of the SU(4) Kondo state; see Fig. 1 (solid line in the right inset). The peak width, which is much broader than that for the SU(2) Kondo model (dotted line), demonstrates the exponential enhancement of the Kondo temperature mentioned above. Another remarkable effect is that the SU(4) Kondo peak shifts away from  $\omega = E_F = 0$  and is pinned at  $\omega \approx T_K^{\text{SU}(4)}$ . This can be understood from the Friedel sum rule [19], which, in this case, gives  $\delta = \pi/4$  for the

scattering phase shift at  $E_F$ . Accordingly, the linear conductance at zero temperature is given by  $\mathcal{G}_0 = 4(e^2/h)\sin^2\delta = 2e^2/h$ . It is interesting to recall that the Friedel sum rule gives the same linear conductance also for the TL SU(2) Kondo model. Thus, neither the enhancement of the Kondo temperature nor the linear conductance can distinguish between the SU(4) and the TL SU(2) Kondo effects. This can only be achieved by studying the influence of a parallel magnetic field, which we do now.

*SU(4) Kondo model at finite field.*—Because of the underlying SU(4) symmetry, the orbital pseudospin should behave the same way as the real spin. In particular, the lift of the pseudospin degeneracy will split the Kondo peak (as long as the lift is larger than the Kondo temperature) just like the Zeeman splitting of the real spin does. The only difference is that the pseudospin is more susceptible to the magnetic field than the real spin since  $\mu_{\text{orb}} \gg \mu_B$  (see above). Therefore, at sufficiently large fields ( $2\Delta_{\text{orb}} \gg \Delta_Z \gg T_K^{\text{SU}(4)}$ ), one has four split-Kondo peaks at  $\omega \approx \pm 2\Delta_{\text{orb}}$  and  $\omega \approx \pm \Delta_Z$ ; see Fig. 1 (left inset). At moderate fields such that  $2\Delta_{\text{orb}} \geq T_K^{\text{SU}(4)} \gg T_K^{\text{SU}(2)} \geq \Delta_Z$ , one can have a three-peak structure; see Fig. 1 (dashed line). The lifted degeneracy in the orbital pseudospin gives two side peaks at  $\omega \approx \pm 2\Delta_{\text{orb}}$ , while the spin still retains a Kondo effect and gives the central peak. The central peak (which is now at  $\omega = 0$ ) corresponds to a conventional SU(2) Kondo effect and hence is much narrower than the central resonance for  $B_{\parallel} = 0$ .

The above features of  $A_{\text{tot}}(\omega)$  at equilibrium are directly reflected in the nonlinear conductance,  $\mathcal{G} \equiv dI/dV$ , an experimentally measurable quantity. The current through

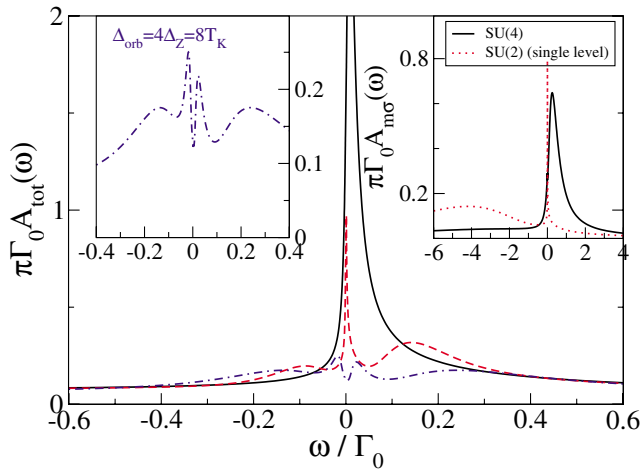


FIG. 1 (color online). NRG results for the total spectral density  $A_{\text{tot}}(\omega)$ . The solid line is for the case of  $\Delta_{\text{orb}} = \Delta_Z = 0$ , the dashed line for  $\Delta_{\text{orb}} = 8T_K^{\text{SU}(4)}$  ( $T_K^{\text{SU}(4)} = 0.0133\Gamma_0$ ) with  $\Delta_Z \approx 0$ , and the dash-dotted line for  $\Delta_{\text{orb}} = 4\Delta_Z = 8T_K^{\text{SU}(4)}$ . (Parameters:  $\epsilon_d = -10\Gamma_0$ ,  $U = 200\Gamma_0$ ,  $\Gamma_0 = 0.01D$ , and  $\delta\Gamma = 0$ .) Left inset: Zoom of the four-peak splitting in  $A_{\text{tot}}(\omega)$ . Right inset: Comparison of the SU(4) (solid line) and the single-level SU(2) (dotted line) Kondo models. (Parameters:  $\epsilon_d = -5\Gamma_0$ ,  $U = 500\Gamma_0$ ,  $\Gamma_0 = 0.02D$ , and  $\delta\Gamma = 0$ .)

the system  $I$  can be expressed in terms of the local DOS [20]:  $I = (e/\hbar)\sum_{\sigma=\uparrow,\downarrow}\sum_{m=1,2}\int d\omega[f_L(\omega) - f_R(\omega)] \times [\Gamma_0(\omega) + \delta\Gamma(\omega)]A_{m\sigma}(\omega)$ , where  $\Gamma_0(\omega) = \pi\rho_0(\omega)|V_0|^2$ ,  $\delta\Gamma(\omega) = \pi\rho_0(\omega)|V_X|^2$ , and  $f_{L(R)}$  is the Fermi function for the left (right) lead. The NRG procedure is valid only at equilibrium, so we need a method capable to produce the nonequilibrium DOS and the nonlinear current. We choose to use a combination of the NCA and the EOM methods [10]. Figures 2(a) and 2(b) display the local DOS and the differential conductance, respectively, for several  $B_{\parallel}$ . We take  $\Delta_{\text{orb}}$  ranging from  $\Delta_{\text{orb}} = 0.5T_K^{\text{SU}(4)}$  to  $\Delta_{\text{orb}} = 1.5T_K^{\text{SU}(4)}$  with  $\mu_{\text{orb}} = 10\mu_B$  leading to  $\Delta_Z = \Delta_{\text{orb}}/5$ . For the lowest magnetic field,  $A_{\text{tot}}(\omega)$  exhibits two splittings, namely, the orbital and the Zeeman splittings with peaks at  $\omega \approx \pm 2\Delta_{\text{orb}}$  and  $\omega \approx \pm \Delta_Z$ , respectively, in excellent agreement with the NRG calculations. As  $\Delta_{\text{orb}}$  increases, a substructure arises in the outer peaks. These new side peaks at  $\omega \approx \pm 2\Delta_{\text{orb}} \pm \Delta_Z$  correspond to the simultaneous *spin-flip interorbital* transitions. Increasing further  $B_{\parallel}$  these side peaks in the DOS get better resolved [21]. All these features are also present in the differential conductance plotted in Fig. 2(b).

*Two-level SU(2) Kondo model at finite field.*—As already shown, both the SU(4) and TL SU(2) Kondo models

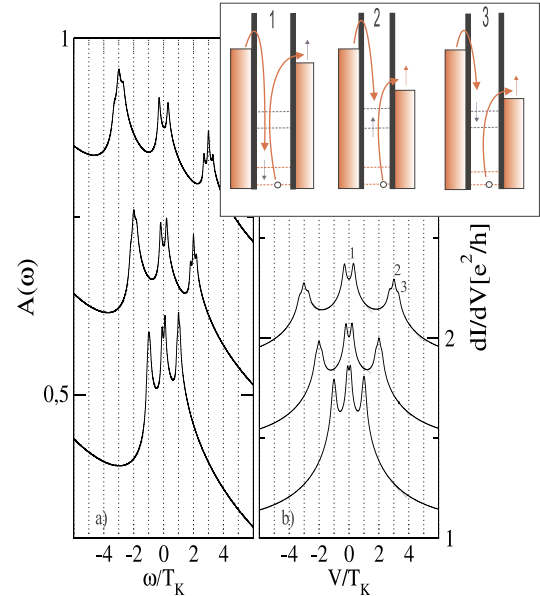


FIG. 2 (color online). NCA + EOM results for the SU(4) Kondo model. (a)  $A_{\text{tot}}(\omega)$  and (b)  $dI/dV$  versus  $eV$  for different magnetic fields ranging from  $\Delta_{\text{orb}} = 0.5T_K^{\text{SU}(4)}$  (bottom curve) to  $\Delta_{\text{orb}} = 1.5T_K^{\text{SU}(4)}$  (top curve). (The curves are shifted vertically for clarity.) When  $B_{\parallel} \neq 0$ , the Kondo resonance splits due to the removal of both spin and orbital degeneracies. The rest of parameters are  $\epsilon_d = -4\Gamma_0$  and  $T = 0.003\Gamma_0$  with  $\delta\Gamma = 0$ . The quantum dot is symmetrically coupled to two leads ( $\Gamma_L = \Gamma_R = \Gamma_0$ ) consisting of Lorentzian bands of width  $2D = 20\Gamma_0$ . Inset: Schematic representation of the allowed transitions. (1) Intraorbital *with spin flip*. (2) Interorbital *without spin flip*. (3) Interorbital *with spin flip*.

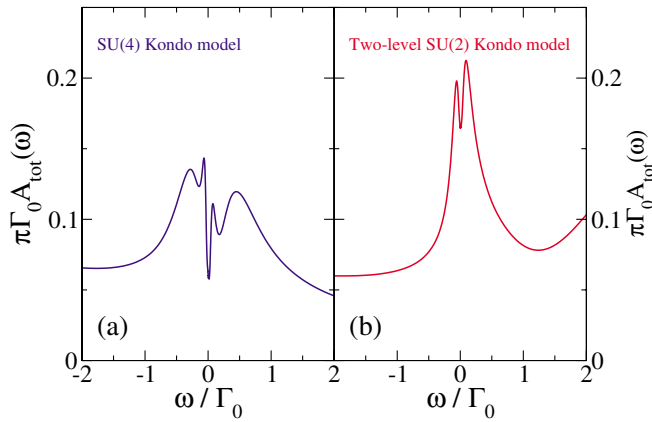


FIG. 3 (color online). NRG results for the total spectral density comparing (a) the SU(4) Kondo model ( $\delta\Gamma = 0$ ) and (b) the two-level SU(2) Kondo model ( $\delta\Gamma = \Gamma_0$ ). Parameters are  $\Delta_{\text{orb}} = 5\Delta_Z = 15T_K^{\text{SU}(4)}$  ( $\approx 0.2\Gamma_0$ ),  $\epsilon_d = -10\Gamma_0$ ,  $U = 1000\Gamma_0$ , and  $\Gamma_0 = 0.01D$ .

lead to similar results for the Kondo temperature and the linear conductance. Nevertheless, the inherent physics is completely different. In the highly symmetric SU(4) Kondo model, the orbital pseudospin and the real spin are indistinguishable (and screened simultaneously at zero field). On the contrary, in less symmetric multiple-level SU(2) Kondo models, the spin should be clearly distinguished from the orbital sector (tunneling processes preserve *only the spin*). This becomes clear at finite magnetic fields: When  $B_{\parallel}$  lifts the orbital degeneracy, only the lower orbital level is occupied so the physics is essentially that of a single-level Kondo model [18]. The Kondo resonance peak gets narrower with increasing  $B_{\parallel}$ . Since  $B_{\parallel}$  also breaks the spin degeneracy, the resulting DOS displays the usual Zeeman splitting. Overall, there are only two peaks around  $E_F$  (Fig. 3).

**Summary.**—We have demonstrated that quantum fluctuations between the orbital and the spin degrees of freedom in NTQDs result in an SU(4) Kondo effect at low temperatures. This exotic Kondo effect manifests as a four-peak splitting in the nonlinear conductance when an axial magnetic field is applied. Similar effects may appear in other systems, such as vertical dots [22] where the orbital quantum number is preserved during tunneling. Recent transport experiments in NTQDs [12] clearly support our theoretical findings.

We thank Pablo Jarillo-Herrero, Silvano de Franceschi, and Leo Kouwenhoven for sharing their experimental results with us prior to publication and for many helpful discussions. We also thank Markus Büttiker, Karyn Le Hur, and David Sánchez for fruitful discussions. This work was supported by the EU RTN No. HPRN-CT-2000-00144, the Spanish MEC and MCyT through Grant No. MAT2002-02465 and the “Ramón y Cajal” program, the SKORE-A, and the eSSC at Postech.

- [1] W. Liang *et al.*, Nature (London) **411**, 665 (2001).
- [2] M. Bockrath *et al.*, Nature (London) **397**, 598 (1999).
- [3] K. Tsukagoshi, B. W. Alphenaar, and H. Ago, Nature (London) **401**, 572 (1999).
- [4] M. Bockrath *et al.*, Science **275**, 1922 (1997); S. J. Tans *et al.*, Nature (London) **394**, 761 (1998).
- [5] W. Liang, M. Bockrath, and H. Park, Phys. Rev. Lett. **88**, 126801 (2002); M. R. Buitelaar *et al.*, Phys. Rev. Lett. **88**, 156801 (2002).
- [6] J. Nygård, D. H. Cobden, and P. E. Lindelof, Nature (London) **408**, 342 (2000); W. Liang *et al.*, *ibid.* **417**, 725 (2002).
- [7] M. R. Buitelaar, T. Nussbaumer, and C. Schönberger, Phys. Rev. Lett. **89**, 256801 (2002); M. R. Gräber *et al.*, cond-mat/0406638.
- [8] K. G. Wilson, Rev. Mod. Phys. **47**, 773 (1975).
- [9] D. C. Langreth and P. Nordlander, Phys. Rev. B **43**, 2541 (1991); N. S. Wingreen and Y. Meir, Phys. Rev. B **49**, 11 040 (1994); M. H. Hettler, J. Kroha, and S. Hershfield, Phys. Rev. B **58**, 5649 (1998).
- [10] We combine occupations obtained from a nonequilibrium  $U \rightarrow \infty$  NCA calculation with an EOM retarded Green function and include the finite lifetime of the intermediate states due to cotunneling at finite voltages and/or magnetic fields. See Y. Meir, N. S. Wingreen, and P. A. Lee, Phys. Rev. Lett. **70**, 2601 (1993).
- [11] Other device geometries have been recently proposed to obtain SU(4) Kondo effect in quantum dots. See L. Borda *et al.*, Phys. Rev. Lett. **90**, 026602 (2003); K. Le Hur and P. Simon, Phys. Rev. B **67**, 201308(R) (2003); G. Zaránd *et al.*, Solid State Commun. **126**, 463 (2003); R. López *et al.*, Phys. Rev. B **71**, 115312 (2005).
- [12] P. Jarillo-Herrero *et al.*, Nature (London) **434**, 484 (2005).
- [13] H. Ajiki and T. Ando, J. Phys. Soc. Jpn. **62**, 1255 (1993).
- [14] E. D. Minot *et al.*, Nature (London) **428**, 536 (2004).
- [15] We are interested in NTQD devices fabricated by depositing metal contacts (for example, Ti/Au) on top of the NT (such as the ones in Ref. [12]). In these samples, the QD is likely coupled to NT electrodes (the electrons tunneling out of the QD enter the NT section underneath the contacts). This “NT-lead–NTQD–NT-lead” structure is also evident in the suspended NT samples of Ref. [14]. There, a suspended nanotube segment (acting as a QD) is coupled to NT leads (the nonsuspended parts).
- [16] M. S. Choi *et al.* (to be published).
- [17] G. Zarand, Phys. Rev. B **52**, 13 459 (1995).
- [18] See also D. Boese, W. Hofstetter, and H. Schoeller, Phys. Rev. B **66**, 125315 (2002).
- [19] D. C. Langreth, Phys. Rev. **150**, 516 (1966).
- [20] Y. Meir and N. S. Wingreen, Phys. Rev. Lett. **68**, 2512 (1992).
- [21] The NRG calculations in equilibrium also show a tiny substructure around the  $\omega \approx \pm 2\Delta_{\text{orb}} \pm \Delta_Z$ , indicating the occurrence of spin-flip interorbital transitions. However, due to the broadening of the outer peaks we are not able to resolve the peaks inside.
- [22] S. Sasaki *et al.*, Phys. Rev. Lett. **93**, 017205 (2004). In this experiment only two peaks, located at  $\omega \approx \pm 2\Delta_{\text{orb}}$ , are resolved in the  $dI/dV$  as the orbital degeneracy is lifted. No signatures of conventional  $S = 1/2$  spin Kondo physics are resolved (probably because  $T > T_K^{\text{SU}(2)}$ ).